

Evolution of Griffith's phase in $\text{La}_{0.4}\text{Bi}_{0.6}\text{Mn}_x\text{Ti}_x\text{O}_3$ perovskite oxide

Vijaylakshmi Dayal, Punith Kumar V., R. L. Hadimani, and D. C. Jiles

Citation: *Journal of Applied Physics* **115**, 17E111 (2014); doi: 10.1063/1.4861205

View online: <http://dx.doi.org/10.1063/1.4861205>

View Table of Contents: <http://scitation.aip.org/content/aip/journal/jap/115/17?ver=pdfcov>

Published by the [AIP Publishing](#)

Articles you may be interested in

[Critical exponents and irreversibility lines of \$\text{La}_{0.9}\text{Sr}_{0.1}\text{CoO}_3\$ single crystal](#)

J. Appl. Phys. **113**, 183909 (2013); 10.1063/1.4804333

[Magnetoelectric coupling in \$\text{La}_{0.6}\text{Ca}_{0.4}\text{MnO}_3\text{-Bi}_{0.6}\text{Nd}_{0.4}\text{TiO}_3\$ composite thin films derived by a chemical solution deposition method](#)

Appl. Phys. Lett. **101**, 212902 (2012); 10.1063/1.4767443

[Incoherent effect of Fe and Ni substitutions in the ferromagnetic-insulator \$\text{La}_{0.6}\text{Bi}_{0.4}\text{MnO}_3\$](#)

J. Appl. Phys. **110**, 073904 (2011); 10.1063/1.3646458

[Spin dynamics and magnetic frustration effects in \$\text{La}_{1-x}\text{Sr}_x\text{CoO}_3\$ \(\$0 < x < 0.5\$ \) compounds](#)

J. Appl. Phys. **97**, 10A509 (2005); 10.1063/1.1855199

[Electronic and magnetic phase diagram of \$\text{La}_{0.5}\text{Sr}_{0.5}\text{Co}_{1-x}\text{Fe}_x\text{O}_3\$ \(\$0 < x < 0.6\$ \) perovskites](#)

J. Appl. Phys. **97**, 10A508 (2005); 10.1063/1.1855197



AIP | Journal of Applied Physics

Journal of Applied Physics is pleased to announce **André Anders** as its new Editor-in-Chief

Evolution of Griffith's phase in $\text{La}_{0.4}\text{Bi}_{0.6}\text{Mn}_{1-x}\text{Ti}_x\text{O}_3$ perovskite oxide

Vijaylakshmi Dayal,^{1,a)} Punith Kumar V.,¹ R. L. Hadimani,² and D. C. Jiles²

¹Department of Physics, Maharaja Institute of Technology-Mysore, Karnataka 571438, India

²Department of Electrical and Computer Engineering, Iowa State University, Ames, Iowa 50011-3060, USA

(Presented 6 November 2013; received 23 September 2013; accepted 15 October 2013; published online 13 January 2014)

Samples of $\text{La}_{0.4}\text{Bi}_{0.6}\text{Mn}_{1-x}\text{Ti}_x\text{O}_3$ have been prepared and their microstructure, composition, and magnetic properties have been investigated for $x = 0.05, 0.1, \text{ and } 0.5$. The deviation in the inverse susceptibility behavior from Curie-Weiss law and increase in susceptibility exponent indicates the evolution of the Griffith's phase in $\text{La}_{0.4}\text{Bi}_{0.6}\text{Mn}_{1-x}\text{Ti}_x\text{O}_3$ around T_C . The presence of Griffith's Phase is inferred due to magnetic frustration with increasing Ti concentration. The deviation between field cooled and zero field cooled magnetization curves is observed in these samples and is attributed to the appearance of the spin glass or cluster glass state that arises due to the magnetic anisotropy. © 2014 AIP Publishing LLC. [<http://dx.doi.org/10.1063/1.4861205>]

INTRODUCTION

Perovskite manganite oxides have attracted considerable attention due to their interesting magnetic ordering and their potential for applications in information storage, such as in spintronic devices and sensors.^{1,2} In recent years, the observation of a Griffith's phase (GP)³ in a number of doped Perovskite manganite oxides⁴ has been reported and is quite interesting. According to Griffith's theory, there is always a finite probability of finding ferromagnetic (FM) clusters with randomly distributed spin [i.e., in paramagnetic (PM) state] in the temperature range $T_C \leq T \leq T_G$, where T_C and T_G are Curie-Weiss temperature and Griffith's temperature, respectively. Bray⁵ extended this explanation to a bond distribution that reduces transition temperature, naming the phase between T_C and T_G , the GP. Thus, GP is the region between the completely ordered states above T_C and the disordered state below T_G . This is the region of PM phase, where FM clusters are formed.

In the completely ordered states below T_C , the spins are ferromagnetically coupled and the temperature dependence of inverse susceptibility (χ^{-1}) generally follows Curie-Weiss law; $\chi^{-1} = C/T - \theta$ and shows linear behaviour in the PM region. Here, θ is the Curie temperature and C is the Curie constant. The GP is typically characterized by a downward deviation from the Curie-Weiss PM behavior in χ^{-1} as the temperature approaches T_C from above. The deviation from Curie-Weiss law in the PM phase can occur due to the increase in magnetic moment arising from the growth of FM spin clusters in the PM region, it then follows the power law relation;⁶ $\chi^{-1} = (T - T_C^R)^{1-\lambda}$ ($0 < \lambda \leq 1$). The power law behavior is a generalized Curie-Weiss law, where the susceptibility exponent λ is a measure of deviation from true Curie-Weiss law and T_C^R which is defined as the characteristic critical temperature of a random ferromagnet.^{7,8}

In this paper, we have analyzed the inverse dc susceptibility (χ^{-1}) in polycrystalline perovskite manganite oxide

$\text{La}_{0.4}\text{Bi}_{0.6}\text{Mn}_{1-x}\text{Ti}_x\text{O}_3$ with $x = 0.05, 0.1, \text{ and } 0.5$ and the occurrence of the GP is studied. The doping of Ti at Mn site in $\text{La}_{0.4}\text{Bi}_{0.6}\text{MnO}_3$ is of particular interest due to the ionic radii of Ti^{4+} (0.605 \AA), which lies in between the ionic radii of the Mn^{3+} (0.64 \AA) and Mn^{4+} (0.54 \AA). The deviation in zero field cooled and field cooled was observed and discussed.

RESULT AND DISCUSSION

Samples of polycrystalline perovskite manganite oxide $\text{La}_{0.4}\text{Bi}_{0.6}\text{Mn}_{1-x}\text{Ti}_x\text{O}_3$ ($x = 0.05, 0.1, \text{ and } 0.5$) were synthesized using conventional solid state reaction method.⁹ All the samples were grown as a single phase which was inferred from X-Ray diffraction data reported elsewhere.¹⁰ Microstructure and composition analysis were carried out using Scanning Electron Microscopy (SEM) and Energy Dispersive X-ray Spectroscopy (EDS), respectively. Figure 1 shows the SEM results of all the compositions under study. The micrograph of the parent sample shows that the grains of the samples are distinct and have well defined boundaries. The sample with $x = 0.05$ had cubic shape grains (Figure 1(a)). For $x = 0.1$, the grains became irregular fractured shapes (Figure 1(b)). For $x = 0.5$, an agglomeration of the grains takes place (Figure 1(c)). We observed here that the grain size decreases with increase in Ti concentration. This behaviour can be attributed to strain induced in the system because of Ti, which blocks the growth of grains. The quantitative analysis of all the compositions from EDS analysis taken on one full grain is given in Table I. We found that all the samples contain all the compositional elements close to the desired values.

The zero field cooled (ZFC) and field cooled (FC) DC magnetization measurement has been carried out at 500 Oe with temperature measured down to 10 K using a SQUID magnetometer as shown in Figure 2(a). We observe here that magnetization decreases with increasing Ti content. A typical maximum exists in the ZFC curve (T_B , the blocking temperature) and at lower temperature ZFC and FC curves diverge significantly for all three samples. This confirms the

^{a)}Author to whom correspondence should be addressed. Electronic mail: drvdayal@gmail.com.

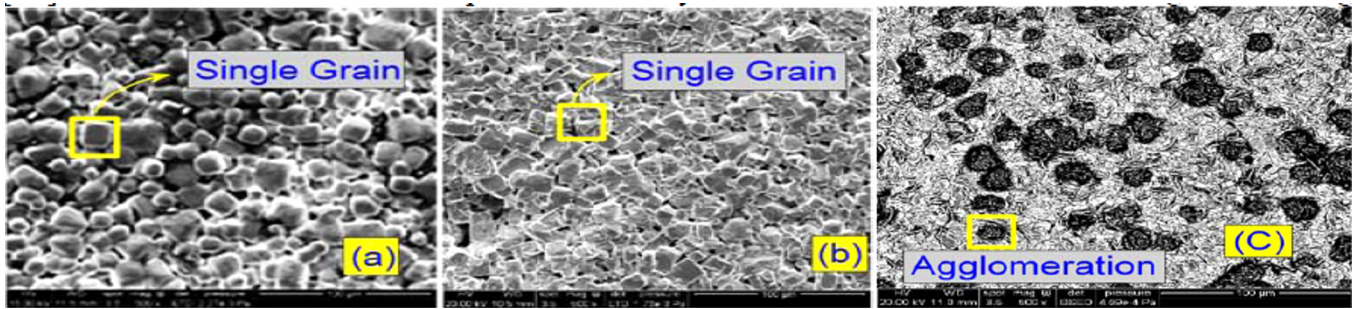


FIG. 1. SEM images from broken pellet at 100 μm resolution for (a) $x=0.05$, (b) $x=0.1$, and (c) $x=0.5$.

TABLE I. Compositions (%) obtained from EDS.

Elements	Line type	$x=0.05$		$x=0.1$		$x=0.5$	
		wt. %	at. %	wt. %	at. %	wt. %	at. %
La	L	22.55	9.05	22.74	9.63	19.28	7.63
Bi	M	41.44	11.05	43.29	12.19	45.28	11.91
Mn	K	17.81	18.07	17.08	18.29	8.77	8.77
Ti	K	0.69	0.81	0.90	1.10	8.70	9.97
O	K	17.51	61.02	15.99	58.79	17.97	61.72
Total		100	100	100	100	100	100

thermomagnetic irreversibility in all the samples. We observed here that T_B shifts to lower temperature with increase in Ti substitution and it is found to be 35 K, 31 K, and 30 K for $x=0.05$, 0.1, and 0.5, respectively. The irreversible temperature (T_{irr}) defined as the temperature below which M_{ZFC} departs from M_{FC} and is found to be 35.7 K, 40.6 K, and 40 K with $x=0.05$, 0.1, and 0.5, respectively, below which large bifurcation starts to occur. Further, we have plotted $\Delta M = M_{\text{FC}} - M_{\text{ZFC}}$ as a function of temperature which vanishes near T_{irr} as shown in Figure 2(b). The plot shows linear behaviour in the temperature range from T_{irr} down to low temperature. Also ΔM increases with increasing Ti content. This confirms that thermomagnetic irreversibility increases with increasing Ti content. Moreover, the drop of ZFC magnetization with the decrease of temperature at the low temperature regime and also the strong irreversibility between ZFC and FC magnetization curves for these samples demonstrate the signature of strong anisotropy (disorder) in the system. The phenomenon of the deviation between FC and ZFC magnetization curves is usually ascribed to the appearance of the spin glass or cluster glass state which arises due to magnetic anisotropy.¹¹ These

can be understood as; when the grain size of a system is reduced, the grain surface region is enhanced compared to interior of the grain mainly due to enhanced surface to volume ratio. At the grain surface, due to the presence of large number of cluster formation, the long range FM order is disturbed and uncompensated spins start to account for large irreversibility.¹² Increase of the net moment of the grains due to the destabilization of the long range FM order at the surface in these systems is strongly dominated by inhomogeneous clusters. Therefore, the decrease in grain size also gives rise to T_B below which the thermal energy cannot overcome the magnetic anisotropy.

The inverse DC susceptibility (χ^{-1}) curve is extracted from DC magnetization measurement with temperature for all the samples and is presented in Figure 3. The curves are fitted with Curie-Weiss law for all the samples given by the equation

$$\chi_{\text{dc}} = N\mu_0\mu_{\text{eff}}^2/3K_B(T - \theta_{\text{CW}}), \quad (1)$$

where N is the calculated value for the number of formula unit (F.U.), μ_{eff} is the effective magnetic moment/F.U., θ_{CW} is the Curie-Weiss temperature, and K_B is Boltzmann's constant.

The estimated values of θ_{CW} obtained by fitting the PM region for χ_{DC}^{-1} vs. temperature along with other obtained parameters are shown in Table II. A linear fit was obtained above T_C for the composition with $x=0.05$ and 0.1 in accordance with the Curie-Weiss law. Whereas for composition with $x=0.5$, a linear fit is obtained well above T_G , where χ_{DC}^{-1} shows a downturn with decreasing temperature, indicating the presence of GP in the temperature range $T_C \leq T \leq T_G$. Further, we have analyzed $\chi_{\text{DC}}^{-1}(T)$ using power law relation $\chi^{-1} = (T - T_C^{\text{R}})^{1-\lambda}$ to investigate the strengthening of

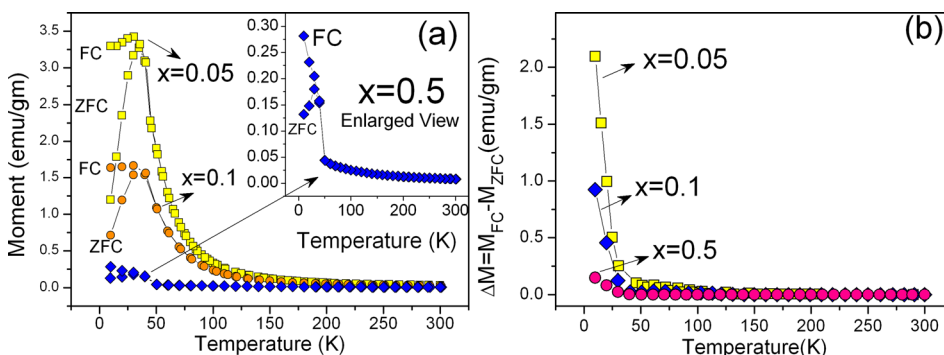


FIG. 2. (a) Zero field cooled and Field cooled DC magnetization measurement at 500 Oe. (b) Plot of $\Delta M = M_{\text{FC}} - M_{\text{ZFC}}$ vs. temperature for all the samples is shown.

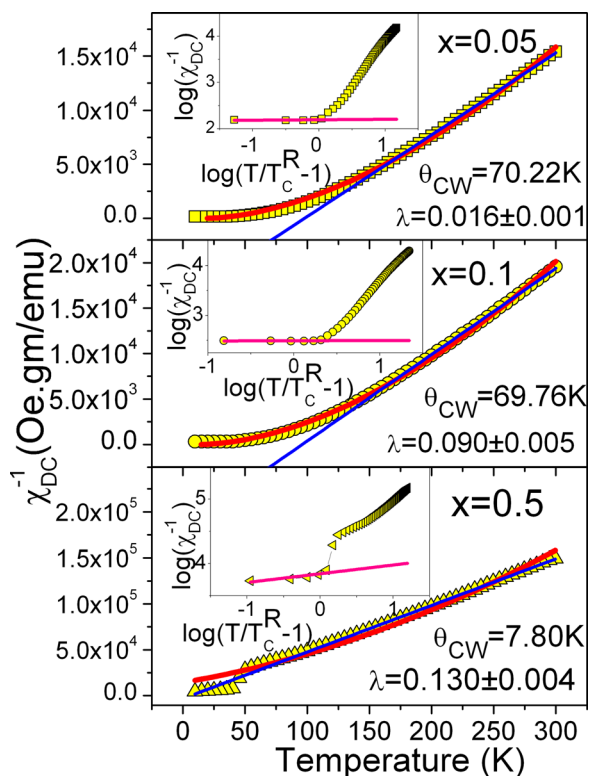


FIG. 3. Temperature dependent inverse Susceptibility for Ti doped samples is shown. Solid red line corresponds to Power Law-Modified Curie-Weiss fit and solid blue line Curie-Weiss fit. The insets show $\log(\chi_{DC}^{-1})$ vs. $\log(T/T_C^R - 1)$ plots under $H = 500$ Oe, where the solid lines (pink) are the linear fittings.

TABLE II. Contains fitted parameters from Figure 3.

Sample	μ_{eff} ($\mu_B/\text{F.U.}$)	T_C (K)	T_C^R (K)	θ_{CW} (K)	λ
x = 0.05	5.6	45	19	70.22	0.016 ± 0.001
x = 0.1	3	45	13	69.76	0.090 ± 0.005
x = 0.5	1.5	40	18	07.80	0.130 ± 0.004

Griffith's Phase with Ti doping. The characteristic temperature T_C^R has been obtained from fitting the χ_{DC}^{-1} vs. temperature in Griffith's regime. The values of λ obtained, which are non-zero and < 1 substantiate the presence of GP.¹³ The value of λ increases with increase in Ti implies the evolution or strengthening of GP phase with doping. As we have observed the magnetization decrease and the thermo-magnetic irreversibility increased (near T_C) with increasing Ti. These facts

suggest that the size of the FM clusters decreases near T_C and that leads to the evolution of GP.

CONCLUSION

The evolution of Griffith's phase with doping of Ti (a non magnetic ion) at the Mn sites of $\text{La}_{0.4}\text{Bi}_{0.6}\text{MnO}_3$ was systematically studied. The increase in the value of susceptibility exponent (λ) with increasing Ti suggests the strengthening of the Griffith's phase in the system. The presence of Griffith's phase due to magnetic in-homogeneity near T_C has been explained.

ACKNOWLEDGMENTS

This work was carried out with the financial aid by Department of Atomic Energy-Board of Research of Nuclear Sciences (DAE-BRNS), India under DAE-Young Scientist research Award to V.D. via project sanction No. 2011/20/37P/01/BRNS/0075. P.K.V. is thankful to DAE-BRNS for providing fellowship. This work was also supported by the Barbara and James Palmer Endowment at the Department of Electrical and Computer Engineering, Iowa State University, USA.

- ¹C. Zener, "Interaction between the d-shells in the transition metals. II ferromagnetic compounds of manganese with perovskite structure," *Phys. Rev.* **82**, 403–405 (1951).
- ²R. Maezono, S. Ishihara, and N. Nagaosa, "Phase diagram of manganese oxides," *Phys. Rev. B* **58**, 11583–11596 (1998).
- ³R. B. Griffith's, *Phys. Rev. Lett.* **23**, 17 (1969), (and references therein).
- ⁴M. Jaime, M. B. Salomon, M. Rubinstein, R. E. Trece, J. Horwitz, and D. B. Chrisey, *Phys. Rev. B* **54**, 11914 (1996).
- ⁵A. J. Bray and M. A. Moore, *J. Phys. C* **15**, L765 (1982), (and references therein).
- ⁶A. K. Pramanik and A. Banerjee, *Phys. Rev. B* **81**, 024431 (2010), (and references therein).
- ⁷M. Sahana, A. Venimadhav, M. S. Hegde, K. Nenkov, U. K. Roler, K. Dorr, and K.-H. Muller, *J. Magn. Magn. Mater.* **260**, 361 (2003).
- ⁸A. H. C. Neto, G. Castilla, and B. A. Jones, *Phys. Rev. Lett.* **81**, 3531–3534 (1998).
- ⁹V. Dayal and S. Keshri, *Solid State Commun.* **142**, 63 (2007).
- ¹⁰V. Dayal, V. P. Kumar, R. L. Hadimani, and D. C. Jiles, "Structural, electrical and Magnetic properties of $\text{La}_{0.4}\text{Bi}_{0.6}\text{Mn}_{1-x}\text{Ti}_x\text{O}_3$ ($x = 0.05, 0.1, 0.5$)," *Phys. Rev. B* (unpublished).
- ¹¹B. D. Cullity, *Introduction to Magnetic Materials* (Addison-Wesley, Reading, MA, 1972), p. 233.
- ¹²S. Kundu and T. K. Nath, *J. Phys.: Condens. Matter* **23**, 356001 (2011), (and references therein).
- ¹³A. J. Bray, *Phys. Rev. Lett.* **59**, 586 (1987), (and references therein).